Polymer Chemistry

PAPER

View Article Online
View Journal | View Issue

Cite this: *Polym. Chem.*, 2015, **6**, 4290

Improved photovoltaic performance of a 2D-conjugated benzodithiophene-based polymer by the side chain engineering of quinoxaline†

Qunping Fan,[a] Manjun Xiao,[a] Yu Liu,*[a] Wenyan Su,[a] Huishan Gao,[a] Hua Tan,[a] Yafei Wang,[a] Gangtie Lei,[a] Renqiang Yang*[b] and Weiguo Zhu*[a]

Received 27th February 2015,
Accepted 3rd May 2015

DOI: 10.1039/c5py00305a

www.rsc.org/polymers

To investigate the influence of side chains of quinoxaline on the photovoltaic performances, a novel D–A-type polymer of **PBDTDT(Qx-3)-T** was synthesized and characterized, in which 5,8-dioctylthienyl substituted benzo[1,2-*b*:4,5-*b*′]dithiophene (BDT-T), thiophene (T) and 6,7-dioctyloxy-2,3-diphenylquinoxaline (Qx-3) were used as the donor (D) unit, π-bridge and acceptor (A) unit, respectively. The resulting polymer exhibited good thermal stability with a high decomposition temperature of 357 °C, a low optical bandgap of 1.78 eV with an absorption onset of 696 nm, a low-lying highest occupied molecular orbital (HOMO) energy level of −5.51 eV, and a high carrier mobility of 2.19×10^{-4} cm^2 V^{-1} s^{-1}. Compared to the reported analogues, polymer solar cells (PSCs) based on **PBDTDT(Qx-3)-T**/$PC_{71}BM$ demonstrated the highest open-circuit voltages (V_{oc}) up to 0.96 V. The maximum power conversion efficiency (PCE) of 6.9% with a V_{oc} of 0.94 V, short-circuit current (J_{sc}) of 11.28 mA cm^{-2} and a fill factor (FF) of 64.7% was obtained with a delicate balance among the above factors for the polymer in PSCs. On the basis of these results, it can be concluded that the appending two octyloxy side chains at 6,7-positions of quinoxaline in the BDT-T-*alt*-DTQx type polymers would be a feasible approach to improve photovoltaic properties.

1. Introduction

As a promising sustainable energy source technology for future, polymer solar cells (PSCs) have recently attracted tremendous interest due to their advantages of low cost, light weight, flexibility, and ease of processing, which leads to the realization of next-generation renewable energy sources.[1–4] To improve photovoltaic performance of PSCs, numerous attempts have been made to develop new solution processable donor–acceptor (D–A)-type polymer donor materials with a narrow optical bandgap.[5–9] More encouragingly, PSCs with high-record power conversion efficiencies (PCEs) up to 10.8% were reported.[10] Despite some remarkable advancements of the polymer donor materials being achieved, some challenges still remain in highly efficient PSCs, especially with respect to the high-lying highest occupied molecular orbital (HOMO) levels that lead to low open-circuit voltages (V_{oc}), narrow absorption spectra that lead to small short-circuit current (J_{sc}), and low carrier mobility that leads to a weak fill factor (FF).[11–13] Based on the previous reports,[11,14–16] the PCEs of the PSCs are proportional to three parameters interplaying each other (V_{oc}, J_{sc} and FF). For example, V_{oc} is mainly related to the energy level between the HOMO of the polymer donor materials and the lowest unoccupied molecular orbital (LUMO) of the fullerene acceptor materials.[11] However, a lower HOMO level of the polymer donor materials would reduce FF, increase optical bandgap and decrease J_{sc}.[11,17] That is, high V_{oc}, J_{sc} and FF are difficult to obtain concurrently.[18] Obviously, a delicate balance among these three factors of the optical bandgap, energy level and carrier mobility is needed *via* sophisticated control over the physical properties of a donor material to achieve higher PCEs in PSC.

Recently, 7,8-dithienyl substituted benzo[1,2-*b*:4,5-*b*′]dithiophene (BDT-T) has been flourishing as an electron donor unit for application in PSCs, due to its relatively large and planar conjugated structure that is favorable for π–π stacking, improvement of carrier transportation and absorption in long wavelengths.[19–25] So far in the literature, a record PCE of 10.2% was obtained in the BDT-T polymer based device by the Hou group.[19] Meanwhile, another effective way to promote the physical properties of the conjugated polymer is to introduce

[a]*College of Chemistry, Xiangtan University, Key Lab of Environment-Friendly Chemistry and Application in Ministry of Education, Xiangtan 411105, China. E-mail: liuyu03b@126.com, zhuwg18@126.comz; Fax: +86-731-58292251; Tel: +86-731-58293377*

[b]*Qingdao Institute of Bioenergy and Bioprocess Technology, Chinese Academy of Sciences, Qingdao 266101, China. E-mail: yangrq@qibebt.ac.cn*

†Electronic supplementary information (ESI) available. See DOI: 10.1039/c5py00305a

conjugating components of quinoxaline derivatives with strong quinoid properties, due to their relatively stable and strong electron withdrawing properties that are conducive to promoting the intramolecular charge transfer (ICT) effect, which endows them with a broader light absorption and enhanced carrier transportation.[26–29] A notable PCE up to 8.0% with J_{sc} of 18.2 mA cm^{-2} was obtained in the quinoxaline-polymer based device by the Chou group.[29] Furthermore, to explore the interactions between the BDT-T and 5,8-dithienylquinoxaline (DTQx) in polymers, there are some exciting reports about the BDT-T-*alt*-DTQx-based polymers recently.[30–34] For instance, Hou *et al.* reported a polymer of **PBDTDTQx-T** with an alternating D–A backbone of BDT-T-*alt*-2,3-di(3-alkyloxyphenyl)-DTQx.[32] To further study the effect of various substituted side chains on the photovoltaic properties of these BDT-T-*alt*-DTQx polymers, our group recently reported two other polymers of **PBDTT-TQ** with an alternating D–A backbone of BDT-T-*alt*-6,7-difluoro-2,3-di(3-alkyloxyphenyl)-DTQx and **PBDTDT(Qx-2)-T** with an alternating D–A backbone of BDTT-*alt*-6,7-dialkyloxy-2,3-di(4-alkyloxyphenyl)-DTQx,[33,34] respectively. Recently, some significant influences of various substituted side chains at 6,7-positions of quinoxaline on PCE of these polymer based devices were also observed, while the phenyl has two alkoxy groups. For example, **PBDTDTQx-T** with two hydrogen atoms at 6,7-positions of quinoxaline was found to show a relatively low V_{oc} of 0.76 V, low J_{sc} of 10.13 mA cm^{-2} and high FF of 64.3% which resulted in a poor PCE of 5.0%.[32] **PBDTT-TQ** with two fluorine atoms at 6,7-positions of quinoxaline was found to display a similarly low V_{oc} of 0.77 V, low FF of 56.0% and high J_{sc} of 13.70 mA cm^{-2} resulting in a moderate PCE of 5.9%.[33] **PBDTDT(Qx-2)-T** with two alkoxy groups at 6,7-positions of quinoxaline was found to indicate a relatively moderate J_{sc} of 10.82 mA cm^{-2}, moderate FF of 61.4% and high V_{oc} up to 0.95 V, which resulted in a maximum PCE of 6.3%.[34] Obviously, these previous studies using conjugated two-dimensional (2-D) side chains on the BDT-T unit as donors and various substituted side chains at 6,7-positions of quinoxaline as acceptors not only can increase the rigidity of the repeating unit, but also improve the performances of PSCs. However, a delicate balance among all these three factors of J_{sc}, V_{oc} and FF has still not been achieved in the BDT-T-*alt*-DTQx type polymer based PSCs.

In this work, a novel D–A-type polymer of **PBDTDT(Qx-3)-T** was synthesized and characterized. As shown in Chart 1, compared to the reported analogic polymers,[32–34] this polymer was just appended with two octyloxy side chains at 6,7-positions of quinoxaline. As reported in the literature, two 6,7-dioctyloxy side chains at quinoxaline twist the polymer main chain somehow, which can reduce the HOMO energy level and improve the V_{oc}.[34–36] Meanwhile, removal of the two alkoxy side chains at phenyl not only promotes the electron withdrawing ability of quinoxaline but also reduces intermolecular steric hindrance, which can broaden the absorption spectrum to enhance the J_{sc} value and improve carrier mobility to increase the FF value of the polymer.[37,38] We expected that the unsubstituted phenyl and two octyloxy side chains instead of two hydrogen or two fluorine atoms at 6,7-positions of quinoxaline are able to improve the photovoltaic properties along with a delicate balance among these three factors of J_{sc}, V_{oc} and FF for their polymers in PSCs due to the above alkyl chain modification on quinoxaline combined effect.

The synthetic routes of **PBDTDT(Qx-3)-T** are shown in Scheme 1. As expected, **PBDTDT(Qx-3)-T** shows a low HOMO energy level of −5.51 eV, narrow optical bandgap of 1.78 eV and high hole mobility of 2.19 × 10^{-4} cm^2 V^{-1} s^{-1}, respectively. PSCs based on the polymer/$PC_{71}BM$ blend presented the highest V_{oc} up to 0.96 V. The highest PCE of 6.9% with a V_{oc} of 0.94 V, J_{sc} of 11.28 mA cm^{-2} and FF of 64.7% was achieved. Obviously, the device shows a delicate balance among the above factors, under the illumination of AM 1.5G,

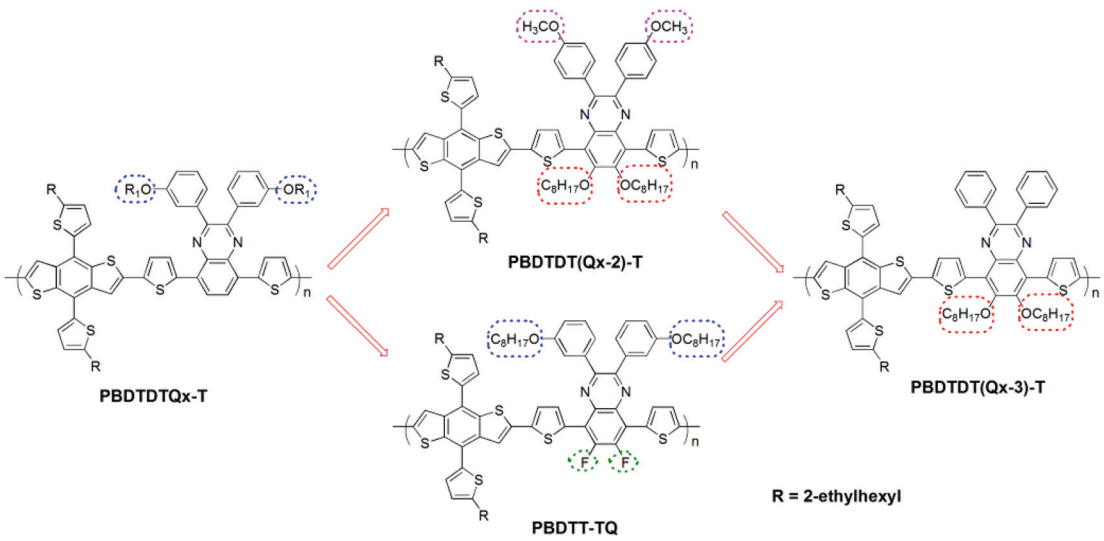

Chart 1 Chemical structures of the BDT-T-*alt*-DTQx based polymers.

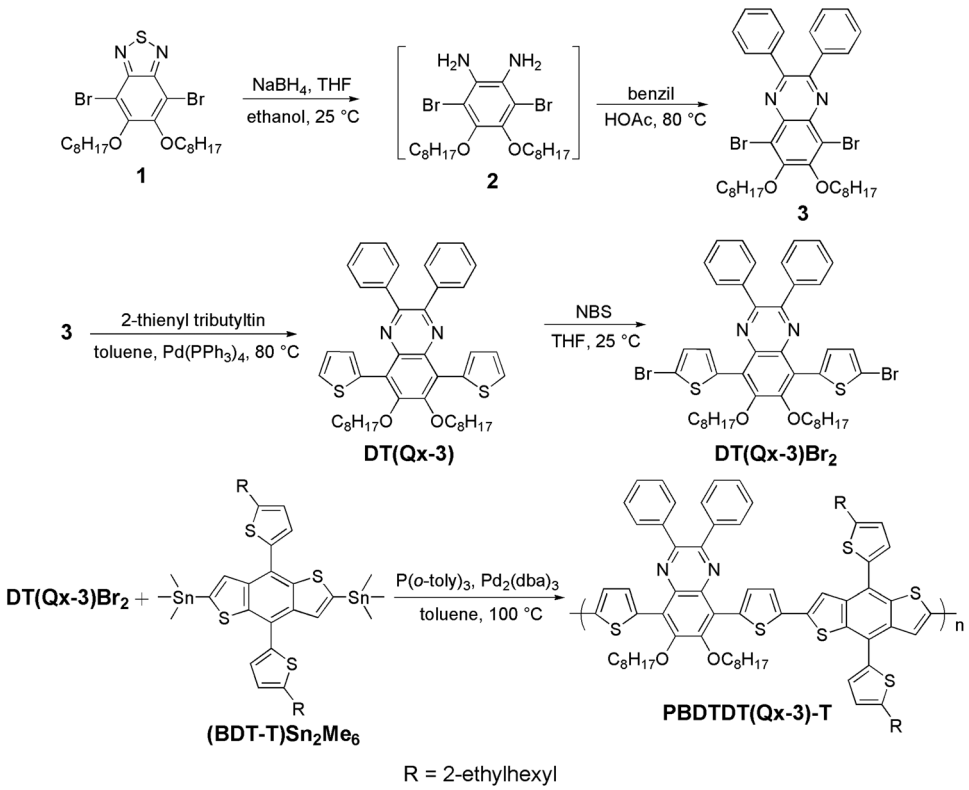

Scheme 1 Synthetic routes for the monomers and **PBDTDT(Qx-3)-T**.

100 mW cm^{-2}. To the best of our knowledge, the maximum PCE and FF values here are higher than those for the previous BDT-T-*alt*-DTQx polymeric derivatives in BHJ-PSCs. This work demonstrates that the photovoltaic properties of the BDT-T-*alt*-DTQx type polymer based PSCs can significantly improve just by grafting two octyloxy side chains at 6,7-positions of quinoxaline.

2. Experimental section

2.1 Materials

Monomer 4,7-dibromo-5,6-bis(octyloxy)benzo[*c*][1,2,5]thiadiazole (**1**) and 2,5-bis(trimethytin)-7,8-bis(5-(2-ethylhexyl)thiophen-2-yl)benzo[1,2-*b*:4,5-*b*′]dithiophene (**(BDT-T)Sn_2Me_6**) were purchased directly from the Suna Tech Inc. The other reagents and chemicals were purchased from commercial sources (Acros, TCI) and used without further purification. Compounds **2**, **3**, **DT(Qx-3)** and **DT(Qx-3)Br_2** were synthesized according to the reported literature.[6,34] The detailed syntheses of monomers and the polymer are presented following the procedures described herein.

2.2 Characterization

Nuclear magnetic resonance (NMR) spectra were recorded on a Bruker AV-400 spectrometer using tetramethylsilane (TMS) as a reference in deuterated chloroform solution at 298 K. Mass spectrometric measurements were performed on Bruker Bifiex III MALDI-TOF. The molecular weights were determined using a Waters GPC 2410 in tetrahydrofuran (THF) *via* a calibration curve of polystyrene as the standard. Thermogravimetric analyses (TGA) were conducted under a dry nitrogen gas flow at a heating rate of 20 °C min^{-1} on a Perkin-Elmer TGA 7. UV-Vis absorption spectra were recorded on a HP-8453 UV visible system. Cyclic voltammograms (CV) were carried out on a CHI660A electrochemical work station with a three electrode electrochemical cell in a 0.1 M tetrabutylammonium hexafluorophosphate ($TBAPF_6$) acetonitrile solution with a scan of 100 mV s^{-1} at room temperature (RT) under an argon atmosphere. In this three-electrode cell, a platinum rod, a platinum wire and a Ag/AgCl electrode were used as a working electrode, a counter electrode and a reference electrode, respectively. The surface morphology of the **PBDTDT(Qx-3)-T**/$PC_{71}BM$ blend film was investigated by atomic force microscopy (AFM) on a Veeco, DI multimode NS-3D apparatus in tapping mode under normal air conditions at RT with a 5 μm scanner.

2.3 Fabrication and characterization of polymer solar cells

The PSCs were fabricated using indium tin oxide (ITO) glass as an anode, Ca/Al as a cathode, and a blend film of the polymer/PCBM as a photosensitive layer. After a 30 nm buffer layer of poly-(3,4-ethylenedioxy-thiophene) and polystyrene sulfonic acid (PEDOT:PSS) was spin-coated onto the precleaned ITO substrate, the photosensitive layer was subsequently prepared

by spin-coating a solution of the **PBDTDT(Qx-3)-T**/$PC_{71}BM$ (1 : 4, w/w) in 1,2-dichlorobenzene (ODCB) on the PEDOT:PSS layer with a typical concentration of 35 mg mL^{-1}, followed by annealing at 80 °C for 10 minutes to remove ODCB. Ca (10 nm) and Al (100 nm) were successively deposited on the photosensitive layer in a vacuum and used as top electrodes. The current–voltage (*I–V*) characterization of the devices was carried out on a computer-controlled Keithley source measurement system. A solar simulator was used as the light source and the light intensity was monitored by a standard Si solar cell. The active area was 1×10^{-2} cm^2 for each cell. The thicknesses of the spun-cast films were recorded by a profilometer (Alpha-Step 200, Tencor Instruments). The external quantum efficiency (EQE) was measured with a Stanford Research Systems model SR830 DSP lock-in amplifier coupled with a WDG3 monochromator and a 150 W xenon lamp.

2.4 Synthesis of the monomers and polymer

2.4.1 5,8-Dibromo-6,7-bis(octyloxy)-2,3-diphenylquinoxaline (3). Compound **1** (0.55 g, 1.00 mmol) and sodium borohydride ($NaBH_4$, 0.57 g, 13.00 mmol) were mixed in ethanol (30 mL) and THF (15 mL) at 0 °C, and stirred for 12 h at RT under a nitrogen atmosphere. After quenching with distilled water (50 mL), the mixture was extracted with anhydrous diethyl ether (20 mL × 3). The combined organic layer was dried over anhydrous magnesium sulfate ($MgSO_4$) and filtered. The filtrate was distilled to remove the solvent and the compound **2** of 2,3-diamino-5,6-bis(octyloxy)-1,4-dibromobenzene was obtained and directly used in the next step. To a solution of compound **2** in ethanol (20 mL) and acetic acid (40 mL) was added benzil (0.27 g, 1.00 mmol). The mixture was refluxed under stirring for 12 h under a nitrogen atmosphere. After cooling to RT and quenching with water, the mixture was extracted with dichloromethane (DCM, 30 mL × 3). The combined organic layer was dried over anhydrous $MgSO_4$ and distilled to remove the solvent. The residue was purified by silica gel column chromatography using a mixed solvent of petroleum ether (PE)–DCM (v/v, 2/1) as an eluent to obtain compound **3** as a yellow solid (0.50 g, 72.1%). ^{1}H NMR (400 MHz, $CDCl_3$, TMS), δ (ppm): 7.64–7.62 (d, J = 7.1 Hz, 4H), 7.39–7.33 (m, 6H), 4.21 (t, J = 6.6 Hz, 4H), 1.94–1.89 (m, 4H), 1.37–1.31 (m, 20H), 0.90 (t, J = 5.3 Hz, 6H). MALDI-TOF MS (*m*/*z*) for $C_{36}H_{44}Br_2N_2O_2$, calcd: 698.17, found: 698.19.

2.4.2 6,7-Bis(octyloxy)-2,3-diphenyl-5,8-di(thiophen-2-yl)-quinoxaline (DT(Qx-3)). To a mixture of compound **3** (0.40 g, 0.57 mmol) and 2-thienyltributyltin (0.85 g, 2.28 mmol) in degassed toluene (30 mL) was added tetrakis(triphenylphosphine)palladium ($Pd(PPh_3)_4$, 0.08 g, 0.07 mmol) and then refluxed for 24 h under a nitrogen atmosphere. After cooling to RT and quenching with water, the mixture was extracted with DCM (20 mL × 3). The combined organic layer was dried over anhydrous $MgSO_4$ and distilled to remove the solvent. The residue was purified by silica gel column chromatography using PE-DCM (v/v, 2/1) as an eluent to obtain **DT(Qx-3)** as a yellow solid (0.35 g, 87.3%). ^{1}H NMR (400 MHz, $CDCl_3$, TMS), δ (ppm): 8.05 (d, J = 3.4 Hz, 2H), 7.66–7.65 (m, 4H), 7.55 (d, J = 5.0 Hz, 2H), 7.33–7.32 (m, 6H), 7.21 (t, J = 8.0 Hz, 2H), 4.04 (t, J = 6.7 Hz, 4H), 1.81–1.76 (m, 4H), 1.40–1.26 (m, 20H), 0.93–0.88 (m, 6H). ^{13}C NMR (100 MHz, $CDCl_3$, TMS), (ppm): 152.87, 150.25, 138.91, 136.41, 133.47, 130.91, 130.33, 128.69, 128.17, 127.89, 126.09, 124.18, 74.10, 31.89, 30.43, 29.52, 29.34, 26.09, 22.71, 14.20. MALDI-TOF MS (*m*/*z*) for $C_{44}H_{50}N_2O_4S_2$, calcd: 704.34, found: 704.45.

2.4.3 5,8-Bis(5-bromothiophen-2-yl)-6,7-bis(octyloxy)-2,3-diphenylquinoxaline (DT(Qx-3)Br_2). To a solution of compound **DT(Qx-3)** (0.30 g, 0.43 mmol) in THF (30 mL) was added *N*-bromosuccinimide (NBS, 0.17 g, 0.95 mmol) in a two-neck round flask. The mixture was then stirred for 4 h at RT. After the solvent was distilled, the residue was purified by silica gel column chromatography using PE-DCM (v/v, 2/1) as an eluent to yield **DT(Qx-3)Br_2** as an orange solid (0.33 g, 90.1%). ^{1}H NMR (400 MHz, $CDCl_3$, TMS), δ (ppm): 7.97 (d, J = 3.9 Hz, 2H), 7.64 (d, J = 6.9 Hz, 4H), 7.37–7.36 (m, 6H), 7.15 (d, J = 3.8 Hz, 2H), 4.08 (t, J = 6.7 Hz, 4H), 1.85–1.81 (m, 4H), 1.43–1.26 (m, 20H), 0.90–0.89 (m, 6H). ^{13}C NMR (100 MHz, $CDCl_3$, TMS), (ppm): 152.68, 150.58, 138.46, 135.89, 135.19, 131.26, 130.34, 128.97, 128.91, 128.27, 123.35, 116.12, 74.23, 31.87, 30.44, 29.50, 29.33, 26.08, 22.72, 14.16. MALDI-TOF MS (*m*/*z*) for $C_{44}H_{48}Br_2N_2O_2S_2$, calcd: 862.15, found: 862.30.

2.4.4 Synthesis of PBDTDT(Qx-3)-T. In a dry 25 mL flask, tris(dibenzylideneacetone)dipalladium ($Pd_2(dba)_3$, 5.0 mg) and tri(*o*-tolyl)phosphine ($P(o\text{-}Tol)_3$, 10.0 mg) were added to a solution of **DT(Qx-3)Br_2** (112 mg, 0.13 mmol) and **(BDT-T)Sn_2Me_6** (100 mg, 0.13 mmol) in 6 mL degassed toluene under a nitrogen atmosphere and stirred vigorously at 100 °C for 16 h. After cooling to RT, the mixture was poured into acetone (100 mL) and the precipitation occurred. It was collected by filtration and successively extracted in Soxhlet apparatus with diethyl ether and chloroform ($CHCl_3$), respectively. The collected $CHCl_3$ solution was concentrated and precipitated with acetone to get a dark solid (135 mg, 81.3%). ^{1}H NMR (400 MHz, $CDCl_3$, TMS), δ (ppm): 8.28–8.19 (br, 2H), 7.81–7.77 (br, 6H), 7.40–8.7.34 (br, 10H), 7.00–6.98 (br, 2H), 4.14–4.13 (br, 4H), 2.95–2.94 (br, 4H), 1.87–1.76 (br, 4H), 1.75–1.73 (br, 2H), 1.48–1.27 (br, 34H), 0.99–0.86 (br, 20H). Anal. Calcd for $C_{78}H_{90}N_2O_2S_6$: C, 73.19; H, 7.09; N, 2.19; S, 15.03. Found: C, 71.32; H, 7.37; N, 2.05; S, 14.71.

3. Results and discussion

3.1 Synthesis and thermal properties

As shown in Scheme 1, compound **2** was prepared through a ring-opening reaction and used immediately to obtain compound **3** *via* the condensation reaction with a yield of 72.1%. Compound **3** was then reacted with 2-thienyltributyltin *via* the Stille coupling reaction to afford **DT(Qx-3)** in the presence of $Pd(PPh_3)_4$ with a moderate yield of 87.3%. **DT(Qx-3)** was brominated with NBS in THF to afford the monomer **DT(Qx-3)Br_2** with a high yield of 90.1%. The polymer of **PBDTDT(Qx-3)-T** was synthesized by palladium-catalyzed Stille polymerization between **DT(Qx-3)Br_2** and **(BDT-T)Sn_2Me_6** with a yield of

Table 1 Molecular weight and thermal properties of **PBDTDT(Qx-3)-T**

Polymers	M_n (kDa)	M_w (kDa)	PDI	Yield (%)	T_d (°C)
PBDTDT(Qx-3)-T	59	97	1.64	81.3	357

81.3%. The chemical structures of compounds **3**, **DT(Qx-3)** and **DT(Qx-3)Br$_2$** were confirmed by ^{1}H NMR, ^{13}C NMR and MALDI-TOF mass spectroscopy (see the ESI†). The molecular weight of the polymer was determined with GPC relative to polystyrene standards. The number average molecular weight (M_n) of 59 kDa with a polydispersity index (PDI) of 1.64 was observed for **PBDTDT(Qx-3)-T**, and the related data are listed in Table 1. Due to the influence of the appending two octyloxy side chains on quinoxaline, **PBDTDT(Qx-3)-T** exhibits excellent solubility in common organic solvents, such as $CHCl_3$, THF, chlorobenzene (CB) and ODCB.

The thermal properties of **PBDTDT(Qx-3)-T** were investigated with thermogravimetric analysis (TGA). As shown in Fig. 1, **PBDTDT(Qx-3)-T** shows excellent thermal stability, with 5% weight-loss at a temperature (T_d) of 357 °C under an inert atmosphere, and its corresponding data are summarized in Table 1.

3.2 Optical properties

The normalized UV-Vis absorption spectra of **PBDTDT(Qx-3)-T** in dilute $CHCl_3$ solution with a concentration of 1×10^{-5} M and a thin film are shown in Fig. 2, and the detailed parameters are summarized in Table 2. Two typical absorption bands are observed in the range of 340–700 nm for the polymer. The high-lying absorption band from 340 to 450 nm is assigned to the π–π* transition, and another low-lying absorption band from 500 to 700 nm should be attributed to the strong ICT interaction between the donor and acceptor units.[9] The absorption of the polymer in the thin film has about 51 nm red-shifted in comparison with the absorption spectra in solution, indicating that the strong aggregation is formed in the thin film. The absorption edge (λ_{onset}) of **PBDTDT(Qx-3)-T** is located at 696 nm in its thin film, corresponding to the optical band gap (E_g^{opt}) of 1.78 eV. Compared to the previous **PBDTDTQx-T** and **PBDTT-TQ** (1.67 and 1.77 eV),[32,33] appending two octyloxy side chains to replace hydrogen or fluorine atoms at 6,7-positions of quinoxaline, can weaken the ICT effect to lead a higher E_g^{opt} value and a higher V_{oc} value in PSCs. A similar phenomenon has also been reported in other studies.[34,36] Furthermore, compared to the previous **PBDTDT(Qx-2)-T** (1.82 eV),[34] two methoxy side chains were eliminated at 4,4′-positions of phenyl in **PBDTDT(Qx-3)-T**, which can enhance the ICT effect to obtain a lower E_g^{opt} value and a higher J_{sc} value.[37,38]

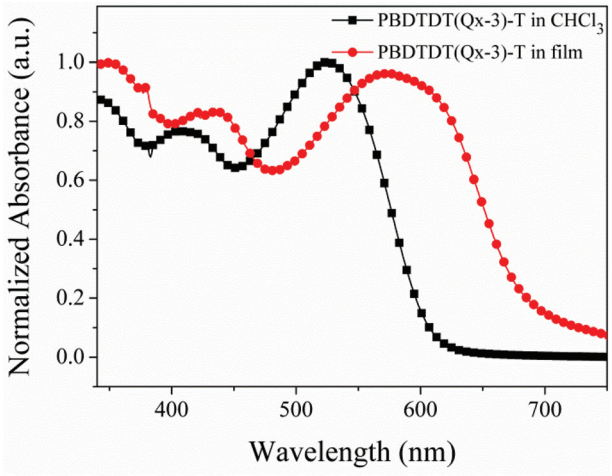

Fig. 2 Normalized UV-Vis absorption spectra of **PBDTDT(Qx-3)-T** in dilute $CHCl_3$ and its neat film at RT.

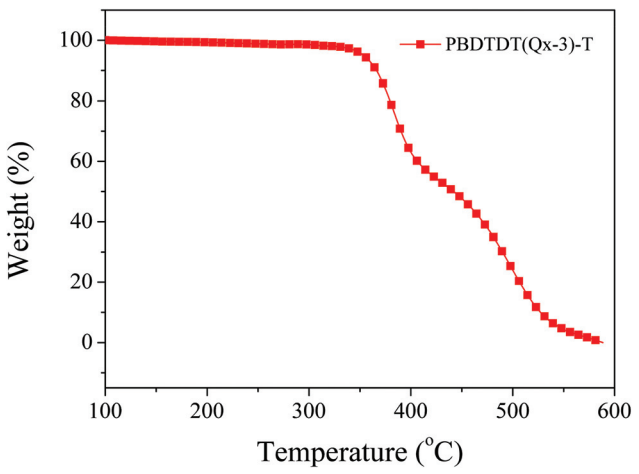

Fig. 1 TGA curve of **PBDTDT(Qx-3)-T** at a scan rate of 20 °C min^{-1} under a nitrogen atmosphere.

3.3 Electrochemical properties

Cyclic voltammetry (CV) was employed to investigate the electrochemical properties of **PBDTDT(Qx-3)-T** by using the Ag/AgCl electrode as a reference and redox potential of ferrocene/ferrocenium (Fc/Fc^+) as the calibrated standard. Fig. 3 shows the recorded CV curve of **PBDTDT(Qx-3)-T**, and the relevant CV data are listed in Table 2. The observed onset oxidation and reduction potentials (E_{ox}/E_{red}) for **PBDTDT(Qx-3)-T** are 1.16 V/−0.78 V, respectively. The HOMO and LUMO energy levels of **PBDTDT(Qx-3)-T** can be calculated according to the empirical equations:[6] $E_{HOMO} = -(E_{ox} - 0.45) - 4.8$ eV, $E_{LUMO} = -(E_{red} - 0.45) - 4.8$ eV and $E_g^{ec} = -(E_{ox} - E_{red})$ eV. As a result, the HOMO and LUMO energy levels (E_{HOMO}/E_{LUMO}) are estimated to be −5.51/−3.57 eV for **PBDTDT-(Qx-3)-T**, respectively. Obviously, **PBDTDT(Qx-3)-T** presents a lower E_{HOMO} value than that of the previous analogues with two alkyloxy groups at phenyl and two fluorine (or hydrogen or octyloxy) at 6,7-positions of quinoxaline,[32–34] Also, increasing two octyloxy side chains at 6,7-positions of quinoxaline can twist the polymer main chain somehow and decreasing two methyloxy side

Table 2 Optical and electrochemical properties of **PBDTDT(Qx-3)-T**

Polymers	λ_{abs} [a]/nm	λ_{abs} [b]/nm	λ_{onset} [b]/nm	E_g^{opt}/eV	E_{HOMO}/eV	E_{LUMO}/eV	E_g^{ec}/eV	Ref.
PBDTDT(Qx-3)-T	408, 526	438, 577	696	1.78	−5.51	−3.57	1.94	This work
PBDTDT(Qx-2)-T	410, 521	420, 564	681	1.82	−5.41	−2.92	2.49	34
PBDTT-TQ	444, 630	447, 601	701	1.77	−5.45	−3.56	1.89	33
PBDTDTQx-T	443, 605	448, 605	740	1.67	−5.12	−3.45	1.67	32

[a] Measured in $CHCl_3$ solution. [b] Measured in the neat film.

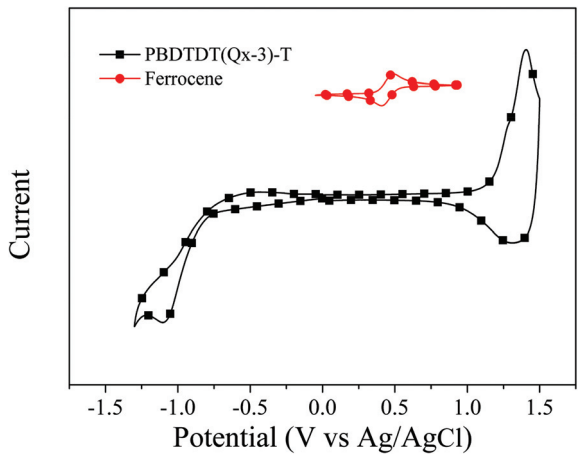

Fig. 3 Cyclic voltammetry curve of **PBDTDT(Qx-3)-T**.

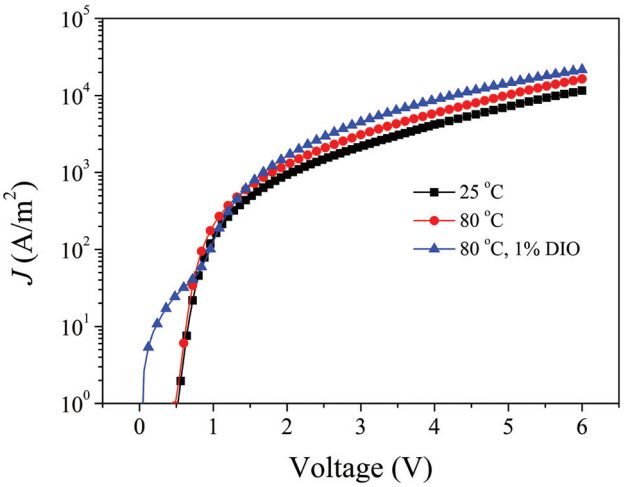

Fig. 4 *J*–*V* curves of the hole **PBDTDT(Qx-3)-T**/$PC_{71}BM$ devices under different conditions.

chains at phenyl can enhance the electron withdrawing ability of quinoxaline causing a lower HOMO level.[34,37] The relatively deep HOMO energy levels (5.51 eV) could be expected to afford higher V_{oc} in PSC applications, which is one of the main contributors to achieve high efficiency PSCs. This discrepancy between the electrochemical and optical bandgaps might be induced by the presence of an energy barrier at the interface between the polymer neat film and the electrode surface.[39]

3.4 Hole mobility

Besides the absorption and energy levels, the charge carrier transport abilities of polymers have also an important effect on the resulting photovoltaic performance of PSCs, especially on FF.[34,40] We measured the hole-only mobilities (μ_h) of **PBDTDT(Qx-3)-T** blended with $PC_{71}BM$ at an optimized blend ratio (w : w, 1 : 4) under different conditions by the space charge limited current (SCLC) method with a device structure of ITO/PEDOT:PSS/polymer:$PC_{71}BM$/Au. The SCLC could be estimated using the Mott–Gurney equation: $J = (9/8)\varepsilon_0\varepsilon_r\mu_h(V/L^3)$,[41] where J is the current density, ε_r is the dielectric constant of polymer, ε_0 is the free-space permittivity (8.85×10^{-12} F m^{-1}), L is the thickness of the blended film layer (105 nm), $V = V_{appl} - V_{bi}$, V is the effective voltage, V_{appl} is the applied voltage, and V_{bi} is the built-in voltage that results from the work function difference between the anode and the cathode. As shown in Fig. 4, the hole-only mobilities of **PBDTDT(Qx-3)-T** are calculated to be 1.01×10^{-4}, 1.53×10^{-4} and 2.19×10^{-4} cm^2 V^{-1} s^{-1} in the hole-only polymer/$PC_{71}BM$-based devices, under without annealing, annealing temperature of 80 °C, and annealing temperature of 80 °C with 1% DIO additive conditions, respectively. Compared to the previous BDT-T-*alt*-DTQx polymers,[32–34] **PBDTDT(Qx-3)-T** shows a best hole mobility under annealing temperature of 80 °C with 1% DIO additive conditions, which implies that a relatively high FF could be obtained in the PSCs.[13,42]

3.5 Photovoltaic properties

To investigate the photovoltaic properties of the polymer, the BHJ-PSCs were also fabricated with a typical device structure of ITO/PEDOT:PSS/active layer/Ca/Al. The active layer of **PBDTDT(Qx-3)-T**/$PC_{71}BM$ with a thickness of 105 nm was obtained from an ODCB solution at a concentration of 35 mg mL^{-1}. The photovoltaic performances of PSCs are strongly affected by the processing parameters,[42] and these processing parameters were investigated to optimize the photovoltaic performance of **PBDTDT(Qx-3)-T**. To obtain the optimal D/A (**PBDTDT(Qx-3)-T**/$PC_{71}BM$, w/w) ratios, annealing temperature, DIO additive concentration and spin-coating rates on the photovoltaic properties, the current density–voltage (*J*–*V*) characteristics of **PBDTDT(Qx-3)-T**/$PC_{71}BM$ based devices at different ratios, annealing temperatures, DIO additives and spin-coating rates are shown in Fig. S1–S4,† respectively. The resulting photovol-

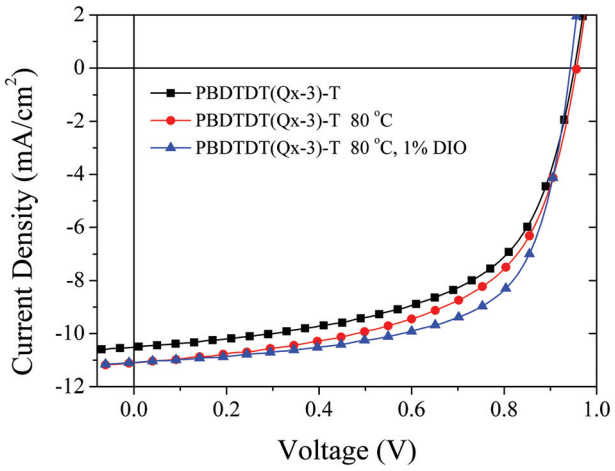

Fig. 5 *J–V* curves of the **PBDTDT(Qx-3)-T**/$PC_{71}BM$-based PSCs at different conditions under illumination of AM1.5G, 100 mW cm^{-2}.

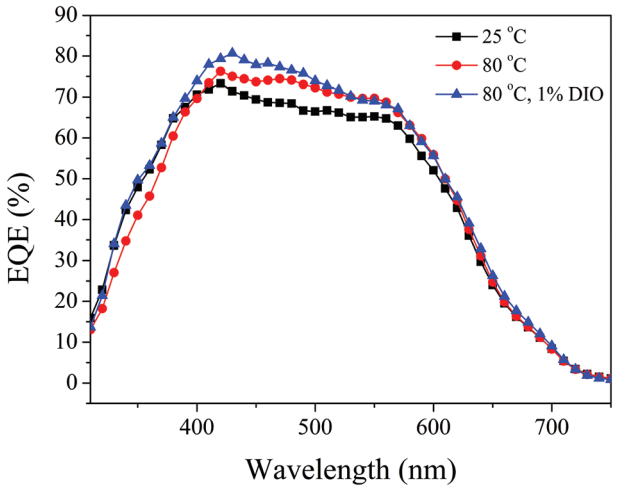

Fig. 6 EQE curves of the **PBDTDT(Qx-3)-T**/$PC_{71}BM$-based devices under different conditions.

taic data are summarized in Tables S1–S4,† respectively. An optimized **PBDTDT-(Qx-3)-T**/$PC_{71}BM$ ratio of 1 : 4, annealing temperature of 80 °C, DIO additive concentration of 1% and spin-coating rate of 2250 rpm were obtained successfully in the BHJ-PSCs. As shown in Fig. 5, three typical devices exhibited the typical *J–V* characteristics under different conditions, and the device parameters, such as J_{sc}, V_{oc}, FF and PCE are summarized in Table 3. More encouragingly, all of the three typical devices exhibit excellent photovoltaic properties.

Without any post fabrication treatment, the device performances exhibited moderate PCE of 5.8%. When we used the annealed active layer, the device performances were moderately improved, which can be attributed to the increased J_{sc} value and well-controlled nanoscale morphology of the BHJ active layer films leading to an improved efficient photoresponse (see Fig. 6 and 7). The corresponding PCE was increased to 6.2% with a comparable V_{oc} value of 0.96 V and a J_{sc} of 11.10 mA cm^{-2}. When further treated with 1% DIO additive, the device performances were greatly enhanced and exhibited a high PCE of 6.9%, which can be attributed to the increased FF value of 64.7% and the same well-optimized nanoscale morphology of the BHJ active layer films leading to an enhanced hole mobility. As result, the maximum PCE of up to 6.9% with a V_{oc} of 0.94 V, a J_{sc} of 11.28 mA cm^{-2} and a FF of 64.7% was obtained in the **PBDTDT(Qx-3)-T**/$PC_{71}BM$-based device. To our knowledge, the recorded maximum PCE and FF values here are higher than those of the previous BDT-T-*alt*-DTQx based on copolymeric derivatives in BHJ-PSCs, due to the side chain modified engineering and the device optimization.[32–34]

To understand why the **PBDTDT(Qx-3)-T**/$PC_{71}BM$ based devices displayed high PCE values, external quantum efficiency (EQE) curves of devices under different conditions were also measured. As depicted in Fig. 6, the **PBDTDT(Qx-3)-T**/$PC_{71}BM$ based three devices show very efficient photoresponse in a broad range from 310 to 730 nm, corresponding to high EQE over 40% in a broad range from 340 to 630 nm is observed for all three devices. The maximum EQE of 73% at 420 nm for the device without annealing, 76% at 422 nm for the device with annealing temperature of 80 °C, and 80% at 431 nm for the device with annealing temperature of 80 °C and 1% DIO additive, was observed respectively. These differences can be attributed to changes of the surface morphologies.[29] Obviously, a high EQE value is responsible for high J_{sc} of **PBDTDT(Qx-3)-T** based PSCs. According to the EQE curves and the solar irradiation spectrum, the integral J_{sc} values of the **PBDTDT(Qx-3)-T** based PSCs are 10.45, 10.96 and

Table 3 Photovoltaic properties of the polymers/$PC_{71}BM$-based PSCs at different conditions, under illumination of AM 1.5G, 100 mW cm^{-2}

Polymers	J_{sc}/mA cm^{-2}	V_{oc}/V	FF/%	PCE_{max}/%	μ_h/cm^2 V^{-1} s^{-1}	Ref.
PBDTDT(Qx-3)-T	10.50	0.95	58.5	5.8	1.01×10^{-4}	This work
PBDTDT(Qx-3)-T[a]	11.10	0.96	58.6	6.2	1.53×10^{-4}	This work
PBDTDT(Qx-3)-T[a,b]	11.28	0.94	64.7	6.9	2.19×10^{-4}	This work
PBDTDT(Qx-2)-T[a]	10.82	0.95	61.4	6.3	1.41×10^{-4}	34
PBDTT-TQ[c]	13.70	0.77	56.0	5.9	1.00×10^{-4}	33
PBDTDTQx-T[d]	10.13	0.76	64.3	5.0	1.04×10^{-4}	32

[a] Annealing at 80 °C. [b] 1% DIO additive. [c] Annealing at 90 °C. [d] Annealing at 120 °C.

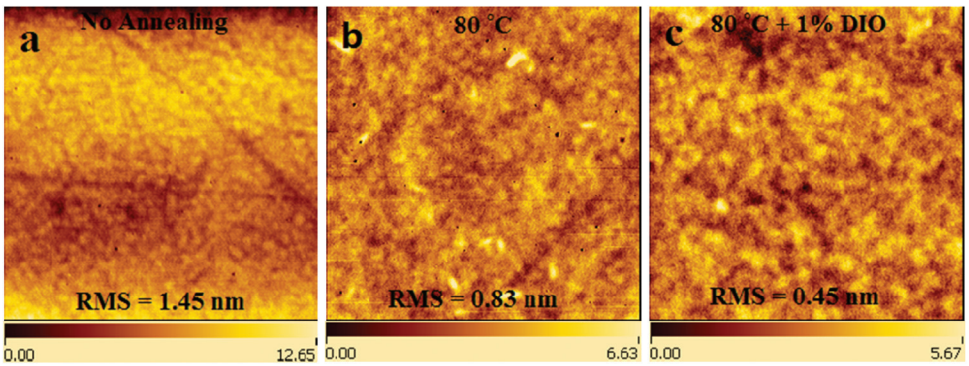

Fig. 7 AFM height images of the **PBDTDT(Qx-3)-T**/$PC_{71}BM$ blend films in unannealed (a), annealed at 80 °C (b), and annealed at 80 °C with % DIO additive (c), respectively.

11.30 mA cm^{-2}, respectively, which are coincident with the measured J_{sc} values within a 2% error.

3.6 Morphology

To better understand the photovoltaic performances of the resulting polymer, tapping mode atomic force microscopy (AFM) measurements are carried out to demonstrate the surface morphologies of the blend films of **PBDTDT(Qx-3)-T**/$PC_{71}BM$ (1 : 4, w/w) processed in unannealed, annealed and annealed with a DIO additive, and the height images (5 × 5 μm^2) are shown in Fig. 6. The root mean square (RMS) roughness is observed to be 1.45 nm in unannealed conditions, and the other blend films after annealing and adding a DIO additive exhibit a smooth surface and the RMS are 0.83 and 0.45 nm, respectively. In general, good surface morphology is available to enhance photovoltaic performance. The results agreed well with the improvement of J_{sc} from 10.50 to 11.28 mA cm^{-2} for the **PBDTDT(Qx-3)-T** based PSCs. Thus, the well-ordered nanoscale morphology of **PBDTDT(Qx-3)T**/$PC_{71}BM$ should also result in high charge carrier mobility, which gives rise to a FF of 64.7%, and a better device performance with a PCE up to 6.9%. Therefore, the relatively excellent morphology together with the high hole mobility mentioned above, results in a high J_{sc} and FF.

4. Conclusions

A novel D–A-type polymer of **PBDTDT(Qx-3)-T** was obtained with a BDT-T-*alt*-DTQx building block to investigate the influence of side chains of quinoxaline on the photovoltaic performances. The polymer exhibited a high decomposition temperature of 357 °C, broad absorption in the range of 300–696 nm, a low-lying HOMO energy level of −5.51 eV, and a high carrier mobility of 2.19×10^{-4} cm^2 V^{-1} s^{-1}. Based on the **PBDTDT(Qx-3)-T**/$PC_{71}BM$ blend, the device exhibited an outstandingly increased V_{oc} value of 0.96 V and a maximum PCE value of 6.9% with a V_{oc} of 0.94 V, a J_{sc} of 11.28 mA cm^{-2}, and a FF of 64.7%. The maximum PCE and FF values here are the highest levels reported in the BDT-T-*alt*-DTQx copolymeric derivatives based PSCs. Our work demonstrates that the photovoltaic properties of the BDT-T-*alt*-DTQx based polymers in PSCs can be remarkably increased by the side chain modified engineering, with just appending two octyloxy side chains at 6,7-positions of quinoxaline.

Acknowledgements

This work was supported by the Major Program for cultivation of the National Natural Science Foundation of China (91233112), the National Natural Science Foundation of China (51273168, 21172187 and 21202139), the Ministry of Science and Technology of China (2010DFA52310), the Innovation Group and Xiangtan Joint Project of Hunan Natural Science Foundation (12JJ7002 and 12JJ8001), the key project of Hunan Provincial Education Department (13A102, 12B123), and the Postgraduate Science Foundation for Innovation in Hunan Province (CX2012B249, CX2013B268). Qunping Fan and Manjun Xiao contributed equally to this work.

Notes and references

1 L. Ye, S. Zhang, L. Huo, M. Zhang and J. Hou, *Acc. Chem. Res.*, 2014, **47**, 1595.
2 P. Bujak, I. K. Bajer, M. Zagorska, V. Maurel, I. Wielgus and A. Pron, *Chem. Soc. Rev.*, 2013, **42**, 8895.
3 Y. Li, *Acc. Chem. Res.*, 2012, **45**, 723.
4 M. Wang, H. Wang, T. Yokoyama, X. Liu, Y. Huang, Y. Zhang, T. Q. Nguyen, S. Aramaki and G. C. Bazan, *J. Am. Chem. Soc.*, 2014, **136**, 12576.
5 J. Yuan, L. Xiao, B. Liu, Y. Li, Y. He, C. Pan and Y. Zou, *J. Mater. Chem. A*, 2013, **1**, 10639.
6 Q. Fan, Y. Liu, M. Xiao, H. Tan, Y. Wang, W. Su, D. Yu, R. Yang and W. Zhu, *Org. Electron.*, 2014, **15**, 3375.
7 D. Ouyang, M. Xiao, D. Zhu, W. Zhu, Z. Du, N. Wang, Y. Zhou, X. Bao and R. Yang, *Polym. Chem.*, 2015, **6**, 55.

8 G. Li, C. Kang, X. Gong, J. Zhang, C. Li, Y. Chen, H. Dong, W. Hu, F. Li and Z. Bo, *Macromolecules*, 2014, **47**, 4645.
9 S. Li, B. Zhao, Z. He, S. Chen, J. Yu, A. Zhong, R. Tang, H. Wu, Q. Li, J. Qin and Z. Li, *J. Mater. Chem. A*, 2013, **1**, 4508.
10 Y. Liu, J. Zhao, Z. Li, C. Mu, W. Ma, H. Hu, K. Jiang, H. Lin, H. Ade and H. Yan, *Nat. Commun.*, 2014, **5**, 6293.
11 J. Warnan, C. Cabanetos, R. Bude, A. E. Labban, L. Li and P. M. Beaujuge, *Chem. Mater.*, 2014, **26**, 2829.
12 J. M. Jiang, H. C. Chen, H. K. Lin, C. M. Yu, S. C. Lan, C. M. Liu and K. H. Wei, *Polym. Chem.*, 2013, **4**, 5321.
13 W. Li, S. Albrecht, L. Yang, S. Roland, J. R. Tumbleston, T. McAfee, L. Yan, M. A. Kelly, H. Ade, D. Neher and W. You, *J. Am. Chem. Soc.*, 2014, **136**, 15566.
14 A. Najari, P. Berrouard, C. Ottone, M. Boivin, Y. Zou, D. Gendron, W. O. Caron, P. Legros, C. N. Allen, S. Sadkin and M. Leclerc, *Macromolecules*, 2012, **45**, 1833.
15 N. I. Abdo, J. Ku, A. A. E. Shehawy, H. S. Shim, J. K. Min, A. A. E. Barbary, Y. H. Jang and J. S. Lee, *J. Mater. Chem. A*, 2013, **1**, 10306.
16 E. T. Hoke, K. Vandewal, J. A. Bartelt, W. R. Mateker, J. D. Douglas, R. Noriega, K. R. Graham, J. M. J. Fréchet, A. Salleo and M. D. McGehee, *Adv. Energy Mater.*, 2013, **3**, 220.
17 H. Li, S. Sun, S. Mhaisalkar, M. T. Zin, Y. M. Lam and A. C. Grimsdale, *J. Mater. Chem. A*, 2014, **2**, 17925.
18 Q. Liu, Z. Du, W. Chen, L. Sun, Y. Chen, M. Sun and R. Yang, *Synth. Met.*, 2013, **178**, 38.
19 S. Q. Zhang, L. Ye, W. C. Zhao, B. Yang, Q. Wang and J. H. Hou, *Sci. China: Chem.*, 2015, **58**, 248.
20 L. Dou, J. Gao, E. Richard, J. You, C. C. Chen, K. C. Cha, Y. He, G. Li and Y. Yang, *J. Am. Chem. Soc.*, 2012, **134**, 10071.
21 L. Ye, S. Zhang, W. Zhao, H. Yao and J. Hou, *Chem. Mater.*, 2014, **26**, 3603.
22 T. Qin, W. Zajaczkowski, W. Pisula, M. Baumgarten, M. Chen, M. Gao, G. Wilson, C. D. Easton, K. Müüllen and S. E. Watkins, *J. Am. Chem. Soc.*, 2014, **136**, 6049.
23 S. H. Liao, H. J. Jhuo, Y. S. Cheng and S. A. Chen, *Adv. Mater.*, 2013, **25**, 4766.
24 Y. Wang, Y. Liu, S. Chen, R. Peng and Z. Ge, *Chem. Mater.*, 2013, **25**, 3196.
25 J. M. Jiang, H. K. Lin, Y. C. Lin, H. C. Chen, S. C. Lan, C. K. Chang and K. H. Wei, *Macromolecules*, 2014, **47**, 70.
26 H. J. Song, D. H. Kim, E. J. Lee and D. K. Moon, *J. Mater. Chem. A*, 2013, **1**, 6010.
27 J. H. Kim, C. E. Song, H. U. Kim, A. C. Grimsdale, S. J. Moon, W. S. Shin, S. K. Choi and D. H. Hwang, *Chem. Mater.*, 2013, **25**, 2722.
28 D. Dang, W. Chen, S. Himmelberger, Q. Tao, A. Lundin, R. Yang, W. Zhu, A. Salleo, C. Müller and E. Wang, *Adv. Energy Mater.*, 2014, **4**, 00680.
29 H. C. Chen, Y. H. Chen, C. C. Liu, Y. C. Chien, S. W. Chou and P. T. Chou, *Chem. Mater.*, 2012, **24**, 4766.
30 H. C. Chen, Y. Chen, C. Liu, Y. H. Hsu, Y. C. Chien, W. T. Chuang, C. Y. Cheng, C. L. Liu, S. W. Chou, S. H. Tung and P. T. Chou, *Polym. Chem.*, 2013, **4**, 3411.
31 M. Tessarolo, D. Gedefaw, M. Bolognesi, F. Liscio, P. Henriksson, W. Zhuang, S. Milita, M. Muccini, E. Wang, M. Seri and M. R. Andersson, *J. Mater. Chem. A*, 2014, **2**, 11162.
32 R. Duan, L. Ye, X. Guo, Y. Huang, P. Wang, S. Zhang, J. Zhang, L. Huo and J. Hou, *Macromolecules*, 2012, **45**, 3032.
33 D. Dang, M. Xiao, P. Zhou, J. Shi, Q. Tao, H. Tan, Y. Wang, X. Bao, Y. Liu, E. Wang, R. Yang and W. Zhu, *Org. Electron.*, 2014, **15**, 2876.
34 W. Su, M. Xiao, Q. Fan, J. Zhong, J. Chen, D. Dang, J. Shi, W. Xiong, X. Duan, H. Tan, Y. Liu and W. Zhu, *Org. Electron.*, 2015, **17**, 129.
35 S. Li, Z. He, J. Yu, S. Chen, A. Zhong, R. Tang, H. Wu, J. Qin and Z. Li, *J. Mater. Chem.*, 2012, **22**, 12523.
36 H. J. Song, D. H. Kim, E. J. Lee, J. R. Haw and D. K. Moon, *Sol. Energy Mater. Sol. Cells*, 2014, **123**, 112.
37 L. J. Lindgren, F. Zhang, M. Andersson, S. Barrau, S. Hellstrom, W. Mammo, E. Perzon, O. Inganas and M. R. Andersson, *Chem. Mater.*, 2009, **21**, 3491.
38 E. Wang, L. Hou, Z. Wang, Z. Ma, S. Hellstr€om, W. Zhuang, F. Zhang, O. Ingan€as and M. R. Andersson, *Macromolecules*, 2011, **44**, 2067.
39 Y. Li, Y. Cao, J. Gao, D. Wang, G. Yu and A. J. Heeger, *Synth. Met.*, 1999, **99**, 243.
40 Z. G. Zhang and Y. F. Li, *Sci. China: Chem.*, 2015, **58**, 192.
41 P. W. M. Blom, V. D. Mihailetchi, L. J. A. Koster and D. E. Markov, *Adv. Mater.*, 2007, **19**, 1551.
42 K. Li, Z. Li, X. Xu, L. Wang and Q. Peng, *J. Am. Chem. Soc.*, 2013, **135**, 13549.

